

Seismic mitigation of substation cable connected equipment using friction pendulum systems

Reza Karami-Mohammadi^{1a}, Masoud Mirtaheri^{1b}, Mojtaba Salkhordeh^{1c}, Erfan Mosaffa^{1d},
Golsa Mahdavi^{2e} and Mohammad Amin Hariri-Ardebili^{*3}

¹Department of Civil Engineering, K.N. Toosi University of Technology, Tehran, Iran

²Department of Civil and Architectural Engineering and Mechanics, University of Arizona, Tucson, Arizona, USA,

³Department of Civil Environmental and Architectural Engineering, University of Colorado, Boulder, USA

(Received September 12, 2019, Revised November 16, 2019, Accepted November 20, 2019)

Abstract. Power transmission substations are susceptible to potential damage under seismic excitations. Two of the major seismic failure modes in substation supplies are: the breakage of brittle insulator, and conductor end fittings. This paper presents efficient isolation strategies for seismically strengthening of a two-item set of equipment including capacitive voltage transformer (CVT) adjacent to a Lightning Arrester (LA). Two different strategies are proposed, Case A: implementation of base isolation at the base of the CVT, while the LA is kept fixed-base, and Case B: implementation of base isolation at the base of the LA, while the CVT is kept fixed-base. Both CVT and LA are connected to each other using a cable during the dynamic excitation. The probabilistic seismic behavior is measured by Incremental Dynamic Analysis (IDA), and a series of appropriate damage states are proposed. Finally, the fragility curves are derived for both the systems. It is found that Friction Pendulum System (FPS) isolator has the potential of decreasing flexural stresses caused by intense ground motions. The research has shown that when the FPS is placed under LA, i.e. Case B (as oppose to Case A), the efficiency of the system is improved in terms of reducing the forces and stresses at the bottom of the porcelain. Several parametric studies are also performed to determine the optimum physical properties of the FPS.

Keywords: friction pendulum system; lightning arrester; capacitor voltage transformer; porcelain breakage; incremental dynamic analysis; fragility curves

1. Introduction

Recent experience obtained from earthquakes has shown that an earthquake poses a major threat to substation equipment (Stearns and Filiatrault 2005). Power outage can remarkably obstruct the rescue operation in the critical time after the disaster. Consequently, substations play an essential role in electric power network (Ashrafi 2003). Having a reliable function in electric power network, power electrical equipment must continue to function immediately after the earthquake (Anagnos 1999). Due to Loma Prieta (1989-USA) and Northridge (1994-USA) earthquakes, over \$280 million damage has been inflicted to the power system facilities (Schiff 1999). During Kocaeli (1999-

Turkey) earthquake, about 14 (7% of total inventory) of Medium Voltage (MV) type and 800 (7% of total inventory) of Medium Voltage/Low Voltage (MV/LV) type Distribution Transformers in the affected areas have experienced heavy damage (Erdik 2000). Loshan 230Kv-substation had received failures of 23 disconnect switches, 11 current transformers, 11 circuit breakers, and 5 post insulators during Manjil (1990-Iran) earthquake (Tavanir 1990). The direct economic loss triggered by Wenchuan (2008-China) earthquake has been estimated over 1 billion dollars and a total number of 246 substation experienced significant damages (Liu *et al.* 2012). Ma and Xie (2018) showed damages imposed to substation's equipment during the 2008 Wenchuan Earthquake. In this event, oil conservator supports were sheared off, all three 550-kV bushings fractured, and leaked transformer oil caused a fire. A lightning arrester failure due to the Fukushima (2011-Japan) earthquake and also leakage in Capacitive Voltage Transformer (CVT) due to the Bam earthquake is shown in Fig. 1-a and Fig. 1-b, respectively. Lopez and Soong (2003) showed that seismic load could result in restraint breakage and excessive absolute acceleration. Recently, isolation techniques have established as a design concept which disengage superstructure from ground shaking. The merit of isolation technique is to increase superstructure safety and significantly reduce probable damages (Charles, A. and Kircher 2012). The period of isolator motion is longer than fixed base structure and the isolator period dominates the

*Corresponding author, Research Associate
E-mail: mohammad.haririardebili@colorado.edu

^a Associate Professor
E-mail: Rkarami@kntu.ac.ir

^b Associate Professor
E-mail: Mmirtaheri@kntu.ac.ir

^c Ph.D. Student
E-mail: M-salkhordeh@email.kntu.ac.ir

^d M.Sc.
E-mail: Emosaffa@mail.kntu.ac.ir

^e Ph.D. Student
E-mail: Golsamahdavi@email.arizona.edu



Fig. 1. a) Damaged lightning arrester after Fukushima earthquake (2011) (Tokyo Electric Power 2011); b) Leakage in capacitive transformer during Bam earthquake (2003) (Karami-Mohammadi *et al.* 2019)

fundamental period of isolated structure. Consequently, the fundamental period of the structure moves away from ground motion predominant period, thereby the energy imposed to the structure will decrease. As the substation facilities have a high rigidity and short displacement, period extension could be a solution to reduce exciting acceleration (Wen *et al.* 2004). Accordingly, in order to strengthening the substation equipment, the use of isolation technology has a great potential to become more prevalent (Saadeghvaziri *et al.* 2009).

In recent decades, detailed research works have been conducted to investigate the effect of isolation techniques in mitigating irreparable damages which may threaten structures. Jeon *et al.* (2015) evaluated the isolation performance of Cone-type Friction Pendulum Bearing System by several numerical analysis. Wang *et al.* (2013) proposed a simple and innovative isolation technique, named Teflon-based lead rubber isolation bearing, to improve the seismic performance of buildings. Also, several research have been conducted to improve the seismic performance of substation's equipment by base isolation technique (Saadeghvaziri *et al.* 2009). Wen *et al.* 2017 investigated the seismic performance of two typical type of Porcelain Electrical Equipment (PEE). They proposed a damping-based method for PEE based on multiple tuned mass dampers to improve the seismic performance of these equipment. Yue *et al.* (2019) proposed a new design process of multiple tuned liquid dampers using the displacement transfer function curves and the equivalent mechanical model of annular tuned liquid damper for seismic reduction of the 1,100-kV composite bushing. Gökçe *et al.* (2019) proposed a new low-cost seismic isolation device that is mounted underneath of HV post insulator to provide period elongation and supplementary damping. Cheng *et al.* (2018) mitigated the seismic risk of cylindrical electrical equipment using a novel isolation device. The device is a circularly arranged lead alloy isolator units installed at the bottom of equipment. Karami and Mosaffa (2018) [20] investigated the workability of FPS isolator to seismic strengthening of electrical equipment. The present research investigates the feasibility of isolation technique to improve

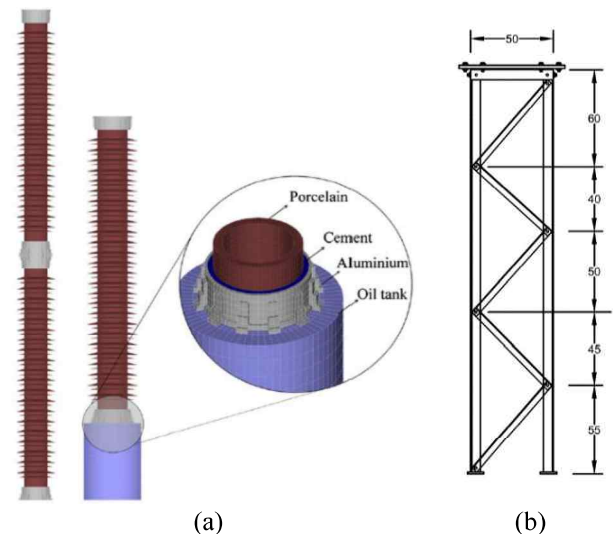


Fig. 2 (a) Different elements of LA and CVT; (b) support structure

the seismic performance of electrical equipment. As it has been mentioned above, the role of Friction Pendulum System (FPS) could be quite effective to prevent failure of CVT and LA. The main goal of this research is to investigate a method such as base isolation technique to improve the seismic performance of such systems. This is done by selecting two various methodology including isolating the CVT while LA is in a fixed position. Consequently, this process is reversed by isolating the LA while the CVT is in a fixed position. Besides, several parametric studies are implemented to determine the optimum characteristics of FPS. Eventually, fragility functions are obtained to determine the probability of failure of equipment set in terms of considered Intensity Measure (IM).

2. Modelling procedure

In this research, it is intended to assess the simultaneous effect of the base isolation and the conductor interaction on

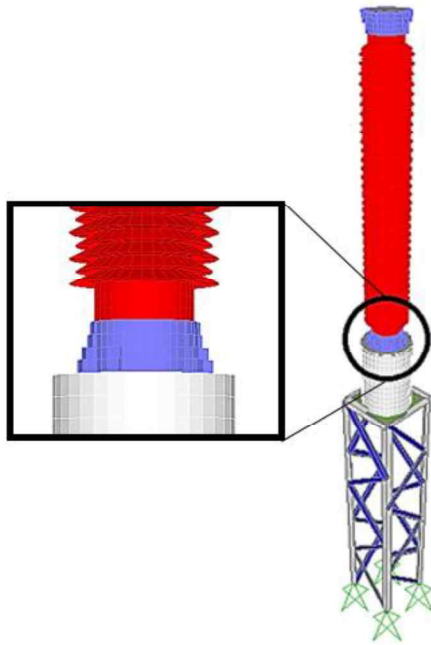


Fig. 3 Finite element model of Capacitive Voltage Transformer (CVT)

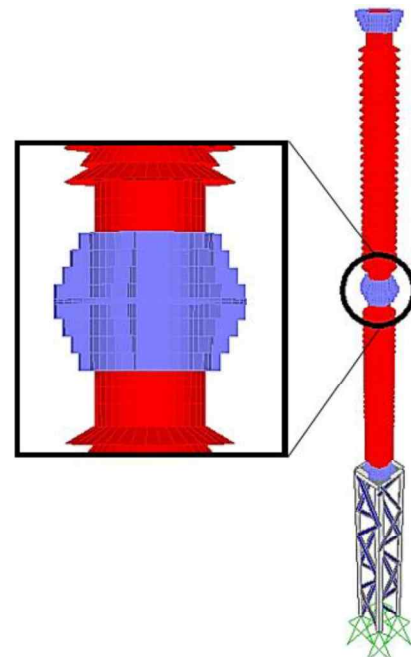


Fig. 4 Finite element model of Lightning Arrester (LA)

Table 1 Mechanical properties of materials

Material	Element Type	Elastic Modulus (MPa)	Poisson Ratio
Aluminum	Shell	69000	0.33
Cement	Shell	25000	0.2
Porcelain	Solid	70000	0.24
Steel	Elastic	210000	0.3

Table 2 Parameters of the modeled equipment

Model	Height (cm)	Total Mass (kg)
CVT Equipment	300	520
CVT Support	250	150
LA Equipment	440	415
LA Support	250	150

Table 3 Details of conductors

Material	Aluminum
Modulus of Elasticity (N/cm^2)	5.72×10^6
Number of layers	5
Number of strings	61
Diameter of strings (cm)	0.432
Total diameter of conductor (cm)	3.92
Cross section area (cm^2)	910
Mass per length (kg/m)	2.509

seismic response of the aforementioned electrical equipment. Therefore, it is essential to model cable-

connected system which is equipped with FPS device. Based on general plan of “MontazerGhaem” substation (Tehran, Iran), the 230 kV LA is installed next to the 230kV CVT at a distance of 3.5m. Therefore, the LA is modeled as well, which is interconnected to the CVT by a flexible conductor on a catenary configuration. Finite element model outputs were carefully examined for different conductor deflections and then compared with the empirical data to ensure that the outputs were reasonable. Different elements of CVT and LA and their support structure are shown in Fig.2-a and Fig.2-b, respectively.

Brittle materials like porcelain insulator and cement fittings are considered to remain in elastic domain. An overview of the material specification is shown in Table 1. Support structure contains a 3D braced truss with 50cm width. Although the higher height of structure will amplify equipment response, according to electrical clearance distance requirements minimum height must not be less than 250cm. The vertical members of support structure are made of L60×60×6 angle while the diagonal ones are made of L40×40×4 angle. Table 2 shows the height and mass of the equipment components. Also, Table 3 shows the parameters required for modelling of conductors.

Modelling procedure is implemented in SAP2000 finite element software. Fig. 3 and Fig. 4 show the CVT and LA model on their corresponding support structure.

In order to have a valid dynamic analysis, dynamic parameters of the models should adjust with the corresponding real equipment. For this purpose, the fundamental period of each modeled equipment is compared to the ones stated in equipment catalog (Table 4). According to Table 4, it is clear that the natural periods of the finite element models have a good agreement with the ones stated in their catalog.

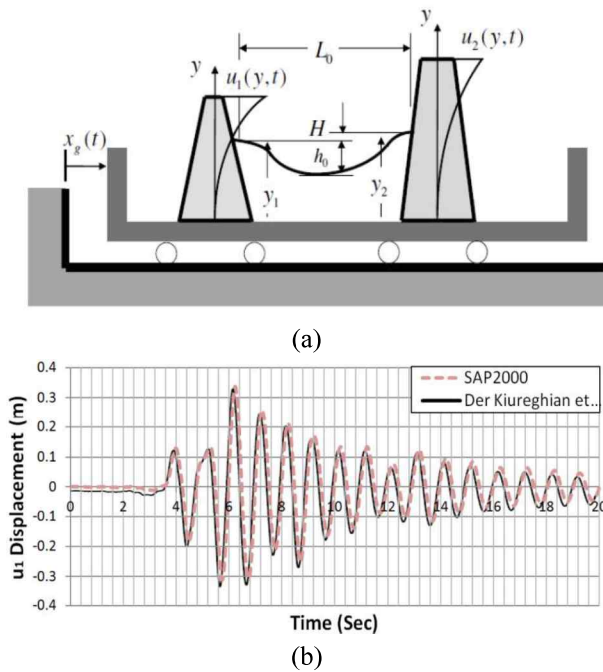


Fig. 5 (a) Stand Alone model (b) Verification result

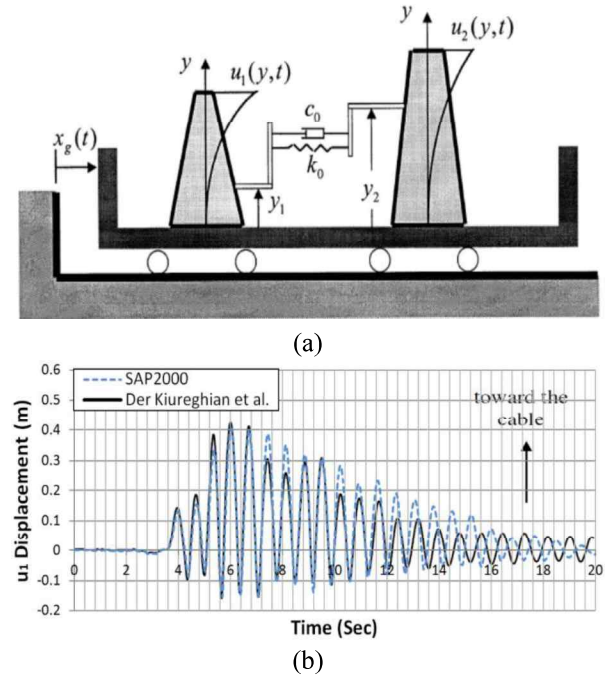


Fig. 6 (a) Conductor connected equipment (b) Verification result

Table 4 Verification of modelling

Description	Natural Period (Catalog) (Sec.)	Natural Period (FEM) (Sec.)	Difference (%)
CVT (Equipment)	0.1124	0.1126	0.17
LA (Equipment)	0.1887	0.1859	1
CVT (on Support Structure)	0.1618	0.1631	0.8
LA (on Support Structure)	-	0.2398	N/A

Interaction of flexible conductors with electrical equipment is a challenge for seismic design of substation's equipment (Dastous and Kiureghian, 2010). Sufficient slack of flexible conductors allows them to provide the required relative displacement without excessive tension (Ghalibafian, 2001). Investigating the required slack of the conductors, a nonlinear spring-dashpot system is considered. This nonlinear model represents the flexibility which is need to model the conductor. It is noteworthy that the flexural rigidity and inertia effects were neglected. According to the experimental test result, force-displacement diagram of cable contains a range of linear elongation and a nonlinear behavior range where their flexibility diminishes and their rigidity increases rapidly. Fig. 5 shows the horizontal traction of a 1796 MCM finite element model compared to the static cyclic test conducted by Dastous and Pierre (1996). As the seismic behavior of cable-connected equipment is the object of this study, as shown in Fig. 5, 6, dynamic behavior of conductors is verified by two simplified models proposed by Kiureghian *et al.* (1999). It should be noted that the mass of DOF 1 and 2 is equal to 1000kg and 500kg, respectively.

In this research, 1796-MCM conductor with uniform distributed weight of 2.509 (kg/m) and modulus of elasticity equal to 5.72×10^4 MPa is used. It is noteworthy that the catenary configuration is used to model the conductors.

IEEE 693 recommended that when the PGA for the 2475-year return period is greater than 0.5g, the high qualification level should be considered. Moreover, it recommends a damping ratio of 2% for substation equipment. Regarding these considerations, spectral acceleration (S_a) is found from Required Response Spectrum (RRS). It is notable that deflections acquired from the RRS should be multiplied by two in order to represent the behavior of equipment in the Performance Level earthquake ($2 \times RRS$). Finally, the minimum length of conductor is computed as 392 cm and 400 cm for fixed-base equipment and isolated-base one, respectively.

The base isolation system should have adequate restoring strength to return the equipment to its original position. Here, a modified friction pendulum system (FPS) possesses sliding and re-centering mechanisms integrated in one unit (Zayas *et al.* 1990). The weight independency trait is the main FPS benefit that makes it appropriate for lightweight device like substation's equipment (Warn and Ryan, 2012). Schematic view of FPS cross section is shown in Fig. 7.

Since impulsive loading may cause fracture of porcelain components, pounding of the slider to stoppers could be a matter of concern. Therefore, the gap size showed in Fig. 7, is one of the momentous parameters considered in this paper. In fact, gap size could control the maximum displacement of the equipment. The efficacy of FPS isolator could be threatened by unwelcome uplift forces which possibility applies damaging effects on the superstructure. Using uplift-restraining isolator could resolve this problem.

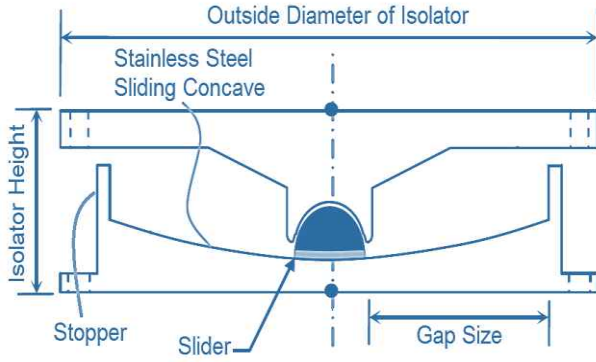


Fig. 7 Schematic view of FPS cross section

Yield strength of the isolator is a function of concave surface material and gravity forces applied to bearing. After yielding, friction behavior will be accompanied by sliding behavior. This causes a combined friction-sliding performance and forms the nonlinear part of force-displacement diagram. Consequently, the strength of the friction pendulum system could be written in the following form

$$F = \mu W \cdot \text{sgn}(\dot{u}) + \frac{W}{R} u \quad (1)$$

In which, W is the weight carried by isolator, R represents the sliding surface radius of curvature, and μ is the friction coefficient of the concave surface. The FPS isolator could fully describe by Coulomb kinetic friction coefficient (μ) and curvature of the isolator ($1/R$). FPS bearing is designed using a two-level procedure, the Design Basis Earthquake (DBE) which is taken as 5% probability of exceedance in 50 years (975-year return period earthquake), and the Maximum Considered Earthquake (MCE) taken as 2% probability of exceedance in 50 years (2475-year return period earthquake). FPS bearing is designed using a two-level procedure, the Design Basis Earthquake (DBE) which is taken as 5% probability of exceedance in 50 years (975-year return period earthquake), and the Maximum Considered Earthquake (MCE) taken as 2% probability of exceedance in 50 years (2475-year return period earthquake). One-second spectral acceleration of site spectrum with 5% of damping for DBE and MCE are equal to $S_{D1}=0.46g$ and $S_{M1}=0.57g$, respectively. As the FPS bearing design is intended for 20% of damping, spectral acceleration values should multiple by 0.8 (Priestley, 1997). The friction coefficient should provide the minimum required force against service loads which is mostly wind load. Additionally, compensating the low weight of equipment and make isolator installation feasible, a 1.5 m \times 1.5 m \times 0.4m concrete block is utilized between the bearings and the foundation of structure which is shown in Fig. 8. As the isolator is installed symmetric, the mass eccentricity of concrete block is negligible. It is noteworthy that dynamic wind loading and minimum friction coefficient is equal to 350kgf and 0.08, respectively.

AASHTO (2003) states two modification factors during the life time of the isolator. The minimum modification factor (λ_{\min}) that is proposed to be equal to one and the

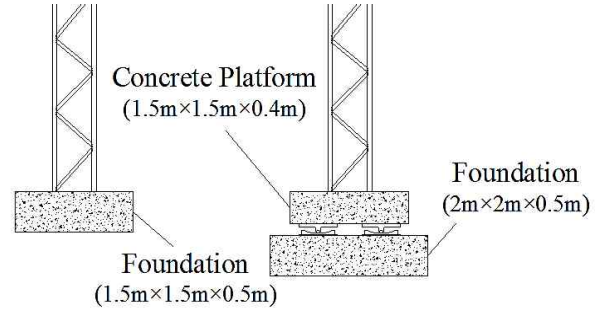


Fig. 8 Schematic view of equipment with isolator

maximum property modification factor that is obtained 1.32. Buckle *et al.* (2006) explained that friction coefficient of the first cycle is roughly 20% greater than the average friction coefficient of all cycles. As a result, the maximum probable friction coefficient is equal to $\mu_{\max} = \mu_{\min} \times 1.2 \times 1.32 = 0.12$. An iterative process is implemented to design FPS isolator according to (AASHTO, 2003; Richins, 2011). The converged target displacement of DBE is 8.1cm. Accordingly, the gap size of FPS, which is shown in Fig. 7, is considered equal to 8.1cm. Reports on the failure mechanism of CVT and LA show that the porcelain insulator breakage outnumbers any other reported failure mechanism. Therefore, this paper focuses on the flexural breakage of porcelain as the main failure mode of these equipment. The ultimate strength of porcelain material (C120) is equal to 500 kg/cm² (IEC 60672-3, 1997). The IEEE 693 defines that the applied stress to the porcelain should not exceed 50% of the ultimate stress of the porcelain. The breakage of fittings, where the flexible conductor connects to the equipment, is considered as the second common failure mode. IEEE Standard 1527 (2006) states that the maximum load which each terminal pad designed for should not exceed 200kg at high qualification level. Moreover, implementation of base isolation technique should not generate any electrical clearance problem. As shown in Fig. 9, safety clearance zones are comprised two phase, ground clearance and the distance between substation ground and bottom of conductor. According to ANSI C37.32 (1996) in a 230-kV substation, the minimum ground clearance should not be less than 2.1m. Since horizontal moving of terminals toward each other can lead to the violation of conductor to the displayed zone in the previous figure, they should be monitored not to exceed 40 cm.

3. Analysis procedure

Assessing the dynamic behavior of high-voltage equipment, triaxial nonlinear time history analysis is implemented. According to the IEEE693, the design load combination is considered accordance to LRFD as follows

$$LRFD : 1.2D + 1.4E_{RSS} + OP \quad (2)$$

Wherein, D represents dead load, E_{RSS} is the earthquake load demand resultant of two perpendicular direction, and OP indicates operating load like tension induced by conductor weight and short circuit force.

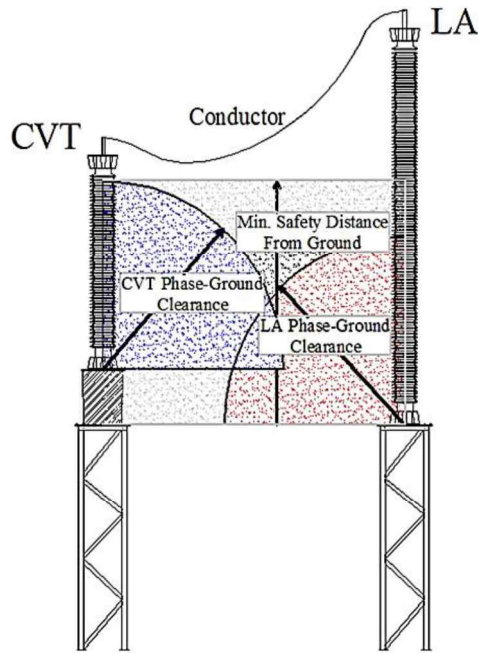


Fig. 9 Schematic view of 2-item set of equipment and essential electrical clearances

Table 5 Earthquake's records selected for dynamic analysis

Earthquake	Station	Distance (km)	PGA (g)
Cape Mendocino	89324 Rio Dell Overpass – FF	18.5	0.385
Chi Chi	TCU047	33.01	0.413
Chi Chi (2)	CHY074	82.49	0.234
Coalinga	36449 Parkfield - Fault Zone 8	29.6	0.131
Imperial Valley	6604 Cerro Prieto	26.5	0.169
Kern County	283 Santa Barbara Courthouse	87	0.127
Kocaeli	Goy nuk	35.5	0.132
Kocaeli (2)	Arcelik	17	0.218
Landers	21081 Amboy	22.5	0.171
Loma Prieta	57504 CoyoteLake Dam (Downst)	21.7	0.179
Loma Prieta (2)	1652 Anderson Dam (Downst)	21.4	0.24
Morgan Hill	57007 Corralitos	22.7	0.109
Morgan Hill (2)	57383 Gilroy Array	11.8	0.292
Northridge	90021 LA - N Westmoreland	29	0.401
Northridge (2)	90015 LA - Chalon Rd	23.7	0.225
San Fernando	24278 Castaic - Old Ridge Route	24.9	0.324
Trinidad	1498 Rio Dell Overpass, FF	71.9	0.147
Victoria	6604 Cerro Prieto	34.8	0.621
Westmorland	5051 Parachute Test Site	24.1	0.242
Whittier Narrows	24157 LA - Baldwin Hills	27	0.142

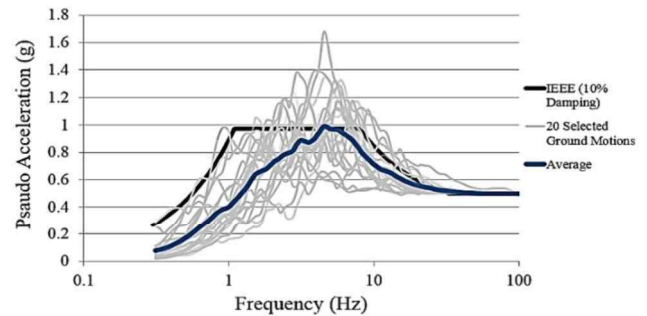


Fig. 10 Ground motions spectrum compared to IEEE std. 693

Twenty far-field earthquake records on very dense soil and rock (Class C site according to ASCE 7-05, 2005) are selected from PEER database. Picked earthquake's characteristics are shown in Table 5.

The spectrum of each selected earthquake comparing to the normalized response spectrum of IEEE 693 is shown in Fig. 10.

Incremental Dynamic Analysis (IDA) is an applicable method to capture the changes of response known as Demand Measure (DM) against increasing ground motion intensity known as Intensity Measure (IM) (Asgarian *et al.* 2012, Vamvatsikos and Cornell 2002). Selecting the best IM for lightweight isolated apparatus, the PGA, PGV, and PGD are the most common indicators of their seismic performance (Akiyama 1985, Davani and Zare 2016, Khorami *et al.* 2017). As the response of the structure mitigated by FPS is a function of its gap size, PGD is selected to represent the seismic behavior of the equipment. Moreover, two aforementioned failure modes (allowable stress at the base of porcelain insulator and allowable force at the terminal pads) are selected as the DM. It is noteworthy that to implement the IDA analysis, SAP2000 is linked to MATLAB software. All repetitive computations are laid into several loops and fed to SAP2000.

4. Results

4.1 The effect of conductors

Median of IDA curves for each equipment, when they are analyzed either alone or connected, is shown in Fig. 11. It should be noted that porcelain breakage failure boundary is displayed by a vertical line. It can be concluded that when two types of equipment are connected, their resistance against PGD will increase. This increases in resistance is more evident in CVT equipment. According Fig. 11-a and Fig. 11-b, it is clear that stress in the porcelain of LA exceeds the ultimate stress at lower PGD comparing to CVT. As a result, the seismic performance of CVT is more appropriate than LA.

4.2 The effect of isolators

Determining the more efficient method to improve the seismic performance of the 2-item set of equipment, the

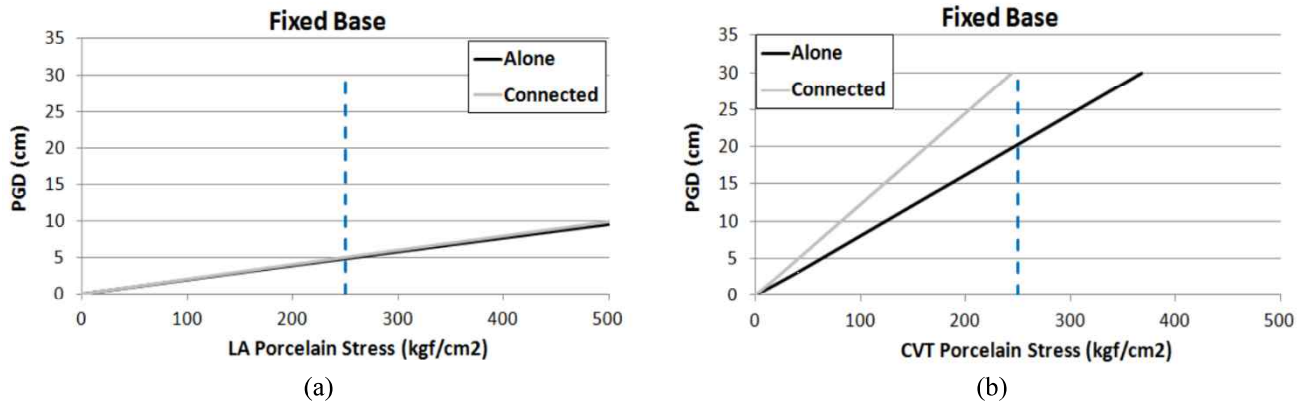


Fig. 11 Effect of conductors on the response of the equipment, (a) LA; (b) CVT

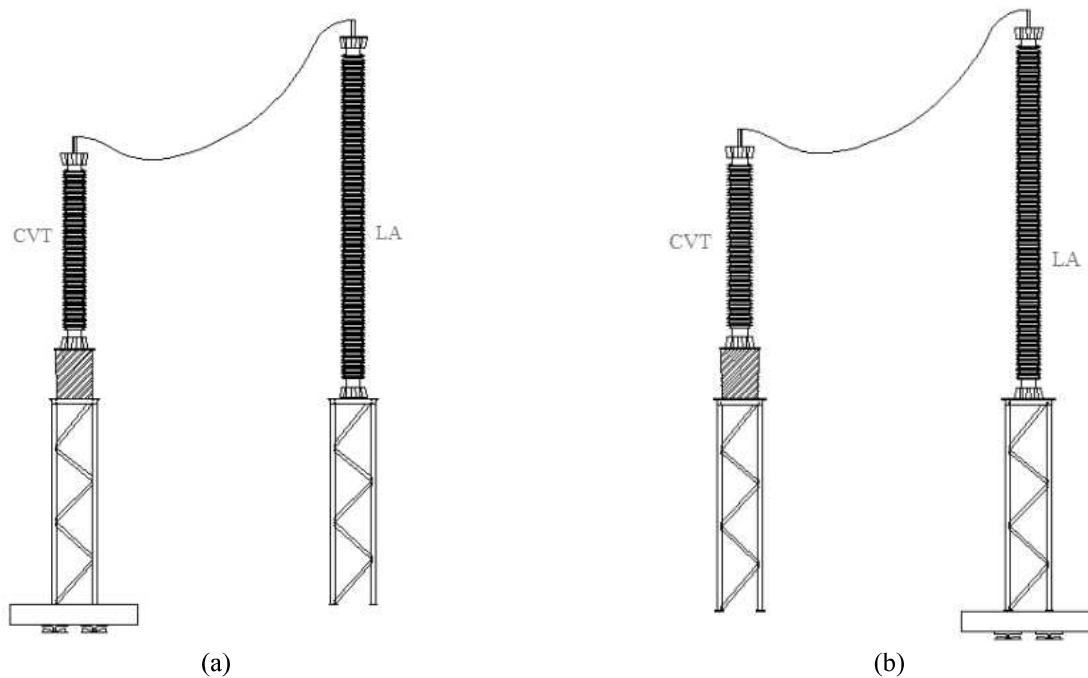


Fig. 12 (a) Base isolation of CVT (b) Base isolation of LA

following two different cases are investigated:

- Base isolation of the CVT while the LA is fixed-base (Fig. 11-a).
- Base isolation of the LA while the CVT is fixed-base (Fig. 11-b)

- Base isolation of the CVT while the LA is fixed-base (Fig. 12-a).
- Base isolation of the LA while the CVT is fixed-base (Fig. 12-b).

Fig. 12 shows the effect of mitigation by these two scenarios on the response of cable connected equipment. As it can be inferred from Fig. 13, when the CVT is mitigated using FPS with a gap size of 8.1cm, the stress in porcelain of CVT will increase suddenly after a threshold of PGD. Also, in this condition, the stress in LA's porcelain does not decrease significantly. On the opposite side, when the FPS isolator is implemented under LA equipment, the stress level in both equipment will decrease. Therefore, isolated-

base LA is more appropriate than fixed-base one, which satisfies stress requirements in both the CVT and LA at all the PGDs. This implies that the LA isolating plan postpones both the LA and CVT failures. Moreover, base isolating of the CVT with a gap size of 8.1cm (case A) cannot improve the seismic performance of 2-item set of equipment and leads to malfunction of isolation plan.

4.3 The effect of gap size

As mentioned before, pounding of sliders to stoppers is a parameter which affects the PGD response. Therefore, the gap size showed in Fig. 7 is an important parameter which considered in this research. Fig. 14-a and 14-b illustrate the effect of the gap size on the response of equipment in both cases. It should be noted that the vertical line shown in this figure is the allowable stress introduced in IEEE693. Fig. 14-c and 14-d show the moment of the bottom of porcelain insulator. It should be noted that these results are the median values obtained from different IDA analysis.

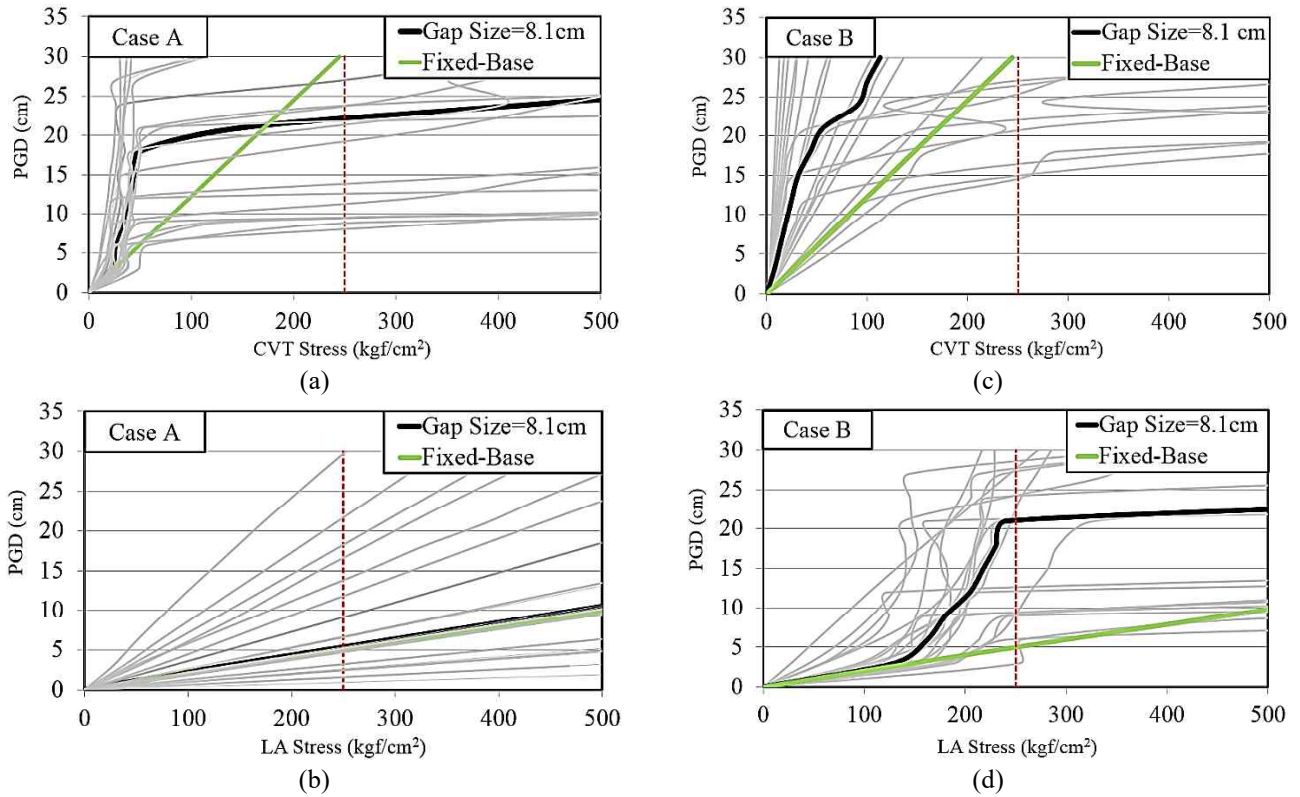


Fig. 13 The effect of base isolation on the response

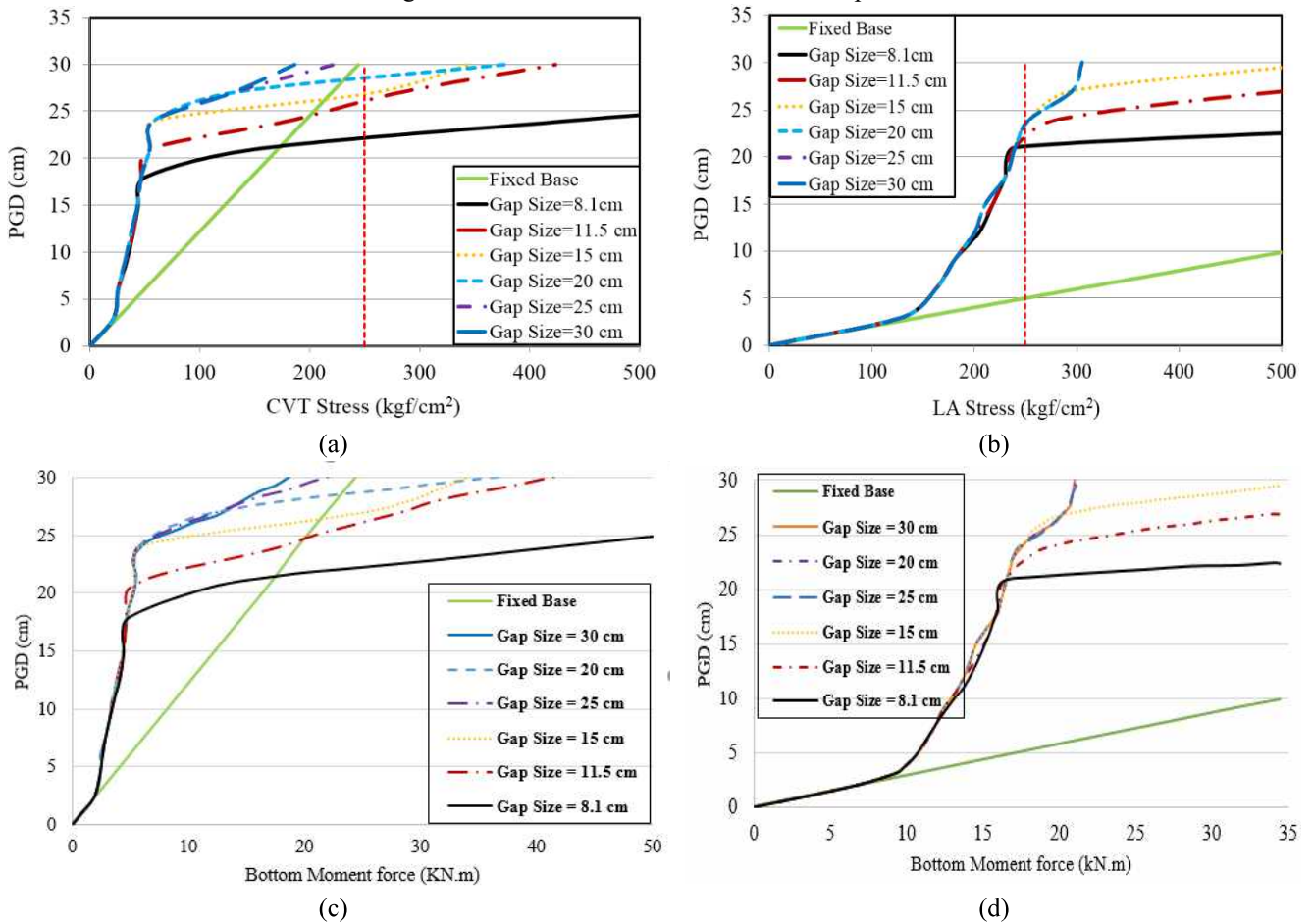


Fig. 14 The effect of different gap size on the response, (a,c) case A; (b,d) case B

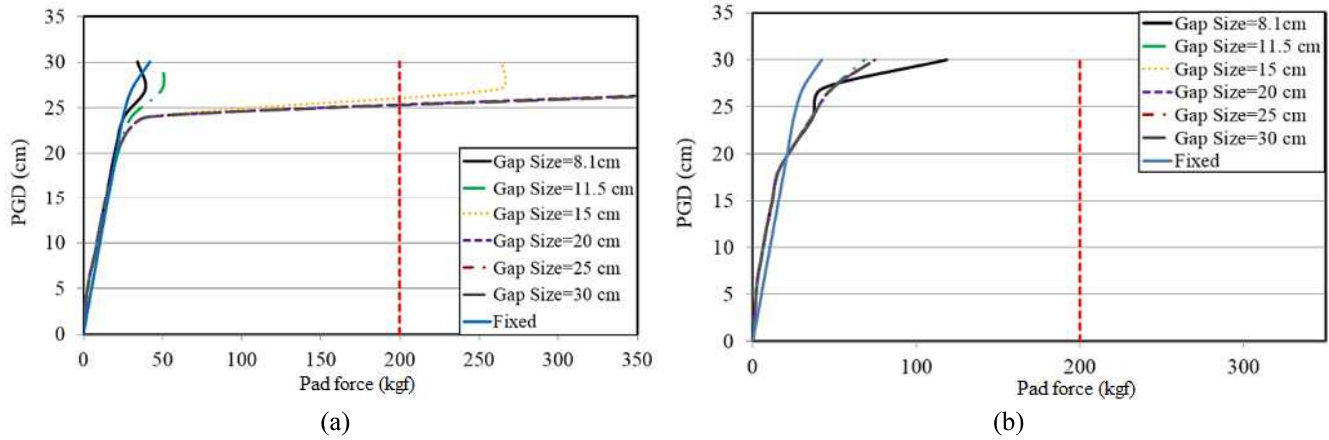


Fig. 15 Median values of terminal pads forces, (a) case A; (b) case B

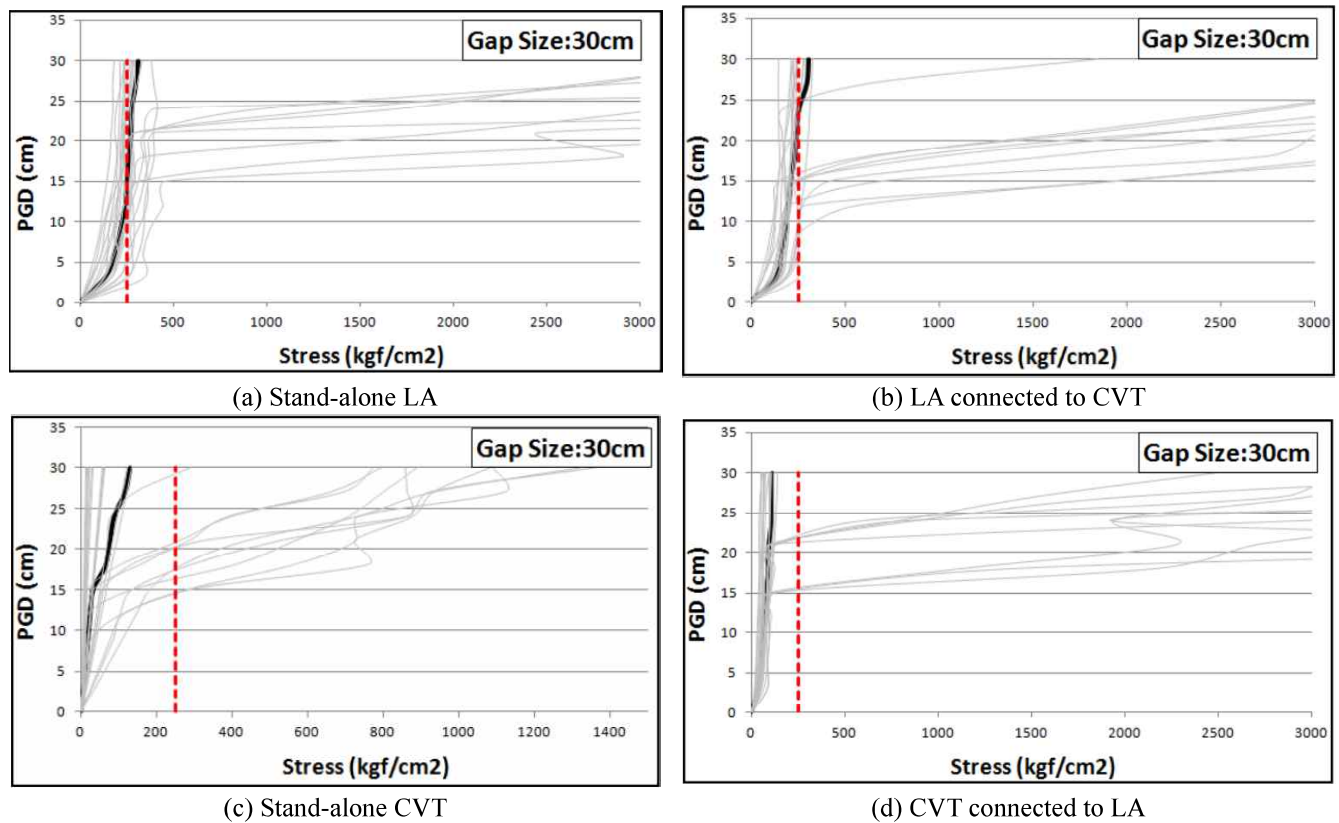


Fig. 16 Effect of conductors

Also, Fig. 15 shows the effect of gap size on the terminal pad forces. Based on IEEE 693, force in terminal pads should not exceed 200 kgf. The vertical line shown in this figure is the allowable force introduced by IEEE 693.

It can be concluded that case A improves the seismic performance of equipment set only for the gap size greater than 25 cm. On the other hand, case B significantly improves the seismic performance of equipment set for all the gap sizes.

4.4 Simultaneous effect of FPS and conductors

In this section, the effect of FPS on the response of equipment either when the 2 types of equipment are

connected or they are stand-alone (for Case B which is the best strategy), is investigated. Fig. 16 shows this problem on the LA and CVT response. Fig. 16-a and 16-b present the stress of the isolated LA porcelain and Fig. 16-c and 16-d illustrate the stress of the isolated CVT porcelain. As a result, conductor have not significant effect on the behavior of equipment isolated by FPS, but as it can be seen when two equipment are connected, isolation technique works slightly efficient as compare to when equipment is stand-alone.

4.5 Controlling of clearance distance

As mentioned in IEEE 693, the minimum distance

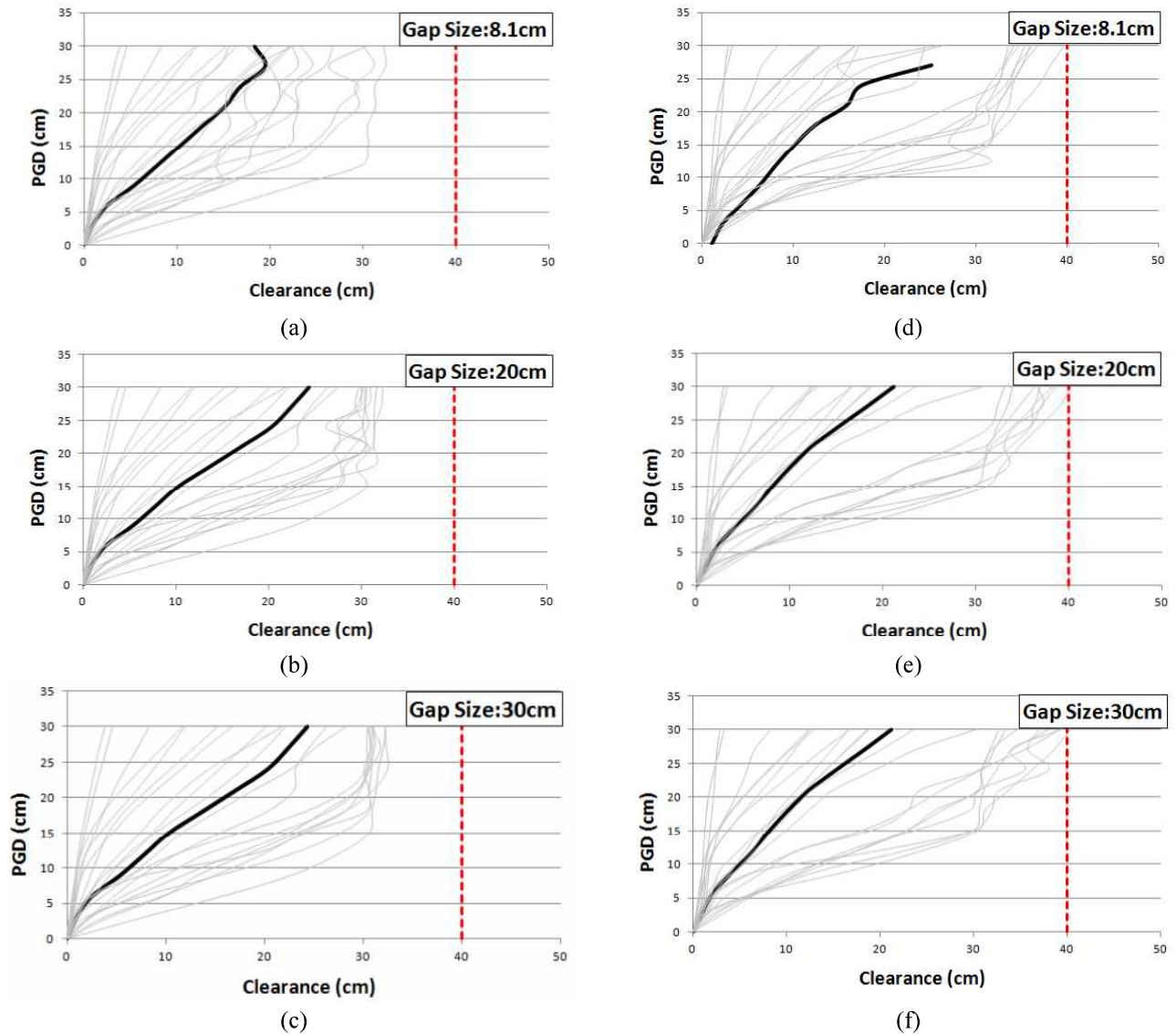


Fig. 17 Clearance distance between CVT and LT, (a) isolation of CVT- gap size 8.1cm; (b) isolation of CVT- gap size 20cm; (c) isolation of CVT- gap size 30cm; (d) isolation of LA- gap size 8.1cm; (e) isolation of LA- gap size 20cm; (f) isolation of LA- gap size 30cm;

between two equipment should not become less than 40cm. In order to control the required clearance distance, relative distance of two equipment is calculated during all analysis. Fig. 17-a to 17-c show the clearance distance between two equipment when CVT is isolated with FPS. Also, Fig. 17-d to 17-f illustrated the clearance distance between two equipment when LA is isolated with FPS. It should be noted that the pale lines are the ground motions result and the solid black line is the median of the response. It is apparent that the required clearance distance never exceeds by isolating of the equipment. Accordingly, utilizing the FPS isolators poses no threaten to required clearance distance between CVT and LT.

4.6 Fragility curves

Fragility functions are used to estimate the probability which a system will tolerate a specified amount of damage during a seismic event (ATC 58, 2007, Waseem and

Spacone 2017). Since the lognormal distribution fits the variety of nonstructural failure data well, it is applied to obtain the fragility functions of the equipment set (Porter and Kiremidjian 2000). Mathematical description of the fragility function is as follows

$$F_i(D) = \Phi\left(\frac{\ln(D/\theta_i)}{\beta_i}\right) \quad (3)$$

In which, $F_i(D)$ is the probability of failure of the component in damage state “i”, Φ represents the standard normal cumulative distribution function, θ_i is the median value, β_i denotes logarithmic standard deviation and D is demand parameter which is defined as the ratio of the maximum response (d_{\max}) to the failure response (d_{failure}).

$$D = \frac{d_{\max}}{d_{\text{failure}}} \quad (4)$$

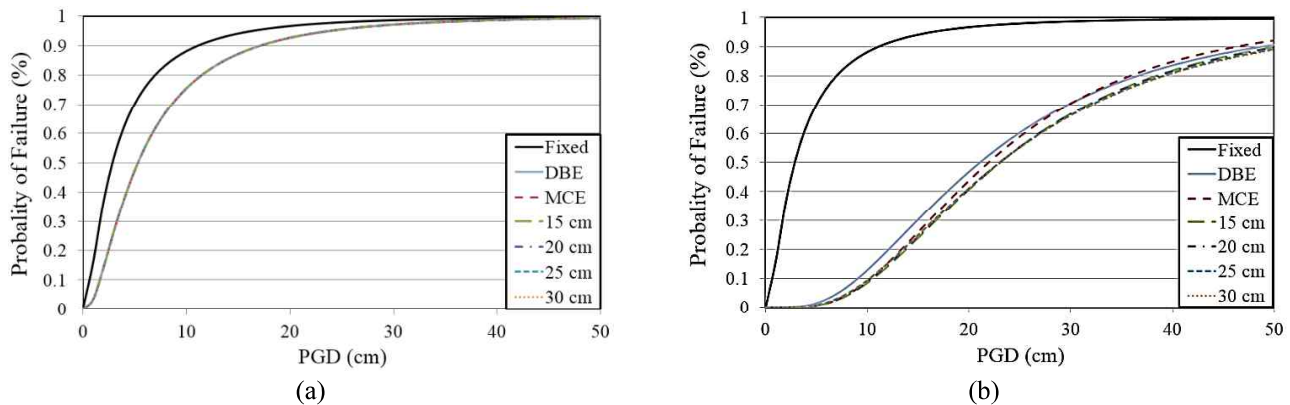


Fig. 18 Fragility functions, (a) case A; (b) case B

Fragility functions developed for two aforementioned cases (case A and B) are shown in Fig. 18.

Fig. 18 affirms that installation of friction pendulum system at the base of LA is more appropriate in order to decrease failure probability of equipment set. Besides, comparing the different gap size state of fragility functions indicates that increasing the stoppers gap sizes will not decrease failure chance of the equipment set. However, seismic response of equipment is slightly improved by increasing the gap size between the FPS stoppers.

5. Conclusion

In this paper, seismic performance of a 2-item set electrical equipment is enhanced using Frictional Pendulum System (FPS). For this purpose, two different procedure, isolation system at the base of CVT (case A) and isolation system at the base of LA (case B), is implemented. Seismic performance of equipment set is assessed using IDA analysis. Thereafter, fragility functions are developed for each equipping procedure. This research has shown in general the usage of base isolation is less effective when they are placed under CVT. However, result show that the effectiveness of same isolation technique is much higher when they are placed under LA. This is an important conclusion in terms of industrial applications. Also, it has been observed from fragility curves that the gap size between the FPS stoppers does not significantly reduce the chance of failure of such systems. This can be used as a guideline in the industry for installing and optimizing the size of FPS. Another important conclusion is that implementing base isolation does not create problem for clearance distance as it has been mentioned in the IEEE 693 standard.

References

- IEEE (2006), *Recommended Practice for Seismic Design of Substations*, The Institute of Electrical and Electronics Engineers, New York, USA.
- AASHTO (2003), *Guide Specifications for Horizontally Curved Steel Girder Highway Bridges with Design Examples for I-girder and Box-girder Bridges*, Washington, DC., USA.
- Akiyama, H. (1985), *Earthquake-Resistant Limit-State Design for Buildings*, University of Tokyo Press, Tokyo, Japan.
- ASCE (2005), *Minimum Design Loads for Buildings and Other Structures*, American Society of Civil Engineers, VA, Reston, USA.
- Anagnos, T. (2001), "Development of an electrical substation equipment performance database for evaluation of equipment fragilities", Pacific Earthquake Engineering Research Center.
- ANSI (American National Standards Institute) (1996), "American National Standard High-Voltage Air Disconnect Switches Interrupter Switches, Fault Initiating Switches, Grounding Switches, Bus Supports and Accessories Control Voltage Ranges-Schedules of Preferred Ratings Construction Guidelines and Specification", Institute of Electrical and Electronics Engineers, <https://doi.org/10.1109/IEEESTD.1996.95627>.
- Applied Technology Council (ATC) (2007), *Guidelines for Seismic Performance: Assessment of Buildings*. Washington D.C., USA.
- Asgarian, B., Khazaee, H. and Mirtaheri, M. (2012), "Performance evaluation of different types of steel moment resisting frames subjected to strong ground motion through incremental dynamic analysis", *J. Steel Struct.*, **12**(3), 363-379, <https://doi.org/10.1007/s13296-012-3006-6>.
- Ashrafi, S.A.H.N. (2003), "Issues of seismic response and retrofit for critical substation equipment", M.Sc. Dissertation, New Jersey Institute of Technology, USA.
- Bai, W., Dai, J., Zhou, H., Yang, Y. and Ning, X. (2017), "Experimental and analytical studies on multiple tuned mass dampers for seismic protection of porcelain electrical equipment", *Earthq. Eng. Eng. Vib.*, **16**(4), 803-813. <https://doi.org/10.1007/s11803-017-0416-7>.
- Buckle, I.G., Constantinou, M.C., Dicleli, M. and Ghasemi, H. (2006), "Seismic Isolation of Highway Bridges", MCEER-06-SP07, Federal Highway Administration, Multidisciplinary Center for Earthquake Engineering Research, State University of New York; USA.
- Cheng, Y., Li, S., Lu, Z., Liu, Z. and Zhu, Z. (2018), "Seismic risk mitigation of cylindrical electrical equipment with a novel isolation device", *Soil Dynam. Earthq. Eng.*, **111**, 41-52. <https://doi.org/10.1016/j.soildyn.2018.04.001>
- Dastous, J.B. and Der Kiureghian, A. (2010), *Application guide for the design of flexible and rigid bus connections between substation equipment subjected to earthquakes*, Pacific Earthquake Engineering Research Center, USA.
- Dastous, J.B. and Pierre, J.H. (1996), "Experimental investigation on the dynamic behavior of flexible conductors between substation equipment during an earthquake", *IEEE Transactions on Power Delivery*, **11**(2), 801-807, <https://doi.org/10.1109/61.489337>.
- Davani, M., Hatami, S. and Zare, A. (2016), "Performance-based

- evaluation of strap-braced cold-formed steel frames using incremental dynamic analysis", *Steel Compos. Struct.*, **21**(6), 1369-1388, <https://doi.org/10.12989/SCS.2016.21.6.1369>.
- Erdik, M. (2000), "Report on 1999 Kocaeli and Duzce (Turkey) earthquakes", Boğaziçi University, Kandilli Observatory and Earthquake Research Institute; Turkey.
- Ghalibafian, H. (2001), "An experimental study on the seismic interaction of flexible conductors with electrical substation equipment", M.Sc. Dissertation, Department of Civil Engineering, The University of British Columbia (UBC), USA.
- Gökçe, T., Yüksel, E. and Orakdöğen, E. (2019), "Seismic performance enhancement of high-voltage post insulators by a polyurethane spring isolation device", *Bullet. Earthq. Eng.*, **17**(3), 1739-1762, <https://doi.org/10.1007/s10518-018-0494-6>.
- IEC 60672-3 (1997), *Ceramic and Glass-Insulating Materials--Part 3: Specifications for Individual Materials*, International Standards and Conformity Assessment for all electrical, electronic and related technologies, Switzerland.
- IEEE Standard 1527 (2006), *IEEE Recommended Practice for the Design of Flexible Buswork Located in Seismically Active Areas*, Institute of Electrical and Electronics Engineers, New York, USA.
- Jeon, B., Chang, S., Kim, S. and Kim, N. (2015), "Base isolation performance of a cone-type friction pendulum bearing system", *Struct. Eng. Mech.*, **53**(2), 227-248, <http://dx.doi.org/10.12989/sem.2015.53.2.227>.
- Karabork, T. (2011), "Performance of multi-storey structures with high damping rubber bearing base isolation systems", *Struct. Eng. Mech.*, **39**(3), 399-410, <https://doi.org/10.12989/sem.2011.39.3.399>.
- Karami-Mohammadi, R., Mirtaheri, M., Salkhordeh, M. and Hariri-Ardebili, M.A. (2019), "A cost-effective neural network-based damage detection procedure for cylindrical equipment", *Adv. Mech. Eng.*, **11**(7), <https://doi.org/10.1177/1687814019866942>.
- Khorami, M., Khorami, M., Motahar, H., Alvansazyazdi, M., Shariati, M. and Jalali, A. (2017), "Evaluation of the seismic performance of special moment frames using incremental nonlinear dynamic analysis", *Struct. Eng. Mech.*, **63**(2), 259-268, <https://doi.org/10.12989/sem.2017.63.2.259>.
- Der Kiureghian, A., Sackman, J.L. and Hong, K.J. (1999), *Interaction in Interconnected Electrical Substation Equipment Subjected to Earthquake Ground Motions*, Pacific Earthquake Engineering Research Center (PEER), CA, USA.
- Liu, R., Zhang, M. and Wu, Y. (2012) "Vulnerability Study of Electric Power Grid in Different Intensity Area in Wenchuan Earthquake", *15th World Conference of Earthquake Engineering (WCEE)*, Lisboa, Portugal, September.
- Lopez Garcia, D. and Soong, T. (2003), "Sliding fragility of block-type non-structural components. Part 1: Unrestrained components", *Earthq. Eng. Struct. Dynam.*, **32**(1), 111-129, <https://doi.org/10.1002/eqe.217>.
- Ma, G.L. and Xie, Q. (2018), "Seismic analysis of a 500-kV power transformer of the type damaged in the 2008 Wenchuan earthquake", *J. Performance Construct. Facilities*, **32**(2), [https://doi.org/10.1061/\(ASCE\)CF.1943-5509.0001145](https://doi.org/10.1061/(ASCE)CF.1943-5509.0001145).
- Mohammadi, R.K. and Mosaffa, E. (2018), "Seismic Rehabilitation of Substation Equipment by Friction Pendulum Systems", *The 2018 Structures Congress*, Incheon, Korea, August.
- FEMA P-751, (2009), "Seismically Isolated Structures, FEMA P-751", *NEHRP Recommended Provisions: Design Examples*, National Institute of Building Sciences, USA.
- Porter, K.A., Kiremidjian, A.S. and LeGrue, J.S. (2001), "Assembly-based vulnerability of buildings and its use in performance evaluation", *Earthq. Spectra*, **17**(2), 291-312, <https://doi.org/10.1193/1.1586176>.
- Tokyo Electric Power (2011), *Report Regarding Collection of Reports pursuant to the Provisions of Article 106, Paragraph 3 of the Electricity Business Act*, Tokyo Electric Power, Tokyo, Japan.
- Priestley, M.N. (1997), "Myths and fallacies in Earthquake Engineering", *Concrete International*, **19**(2), 54-63, <https://doi.org/10.14359/983>.
- Richins, B.D. (2011), "Evaluation and seismically isolated substructure redesign of a typical multi-span pre-stressed concrete girder highway bridge", M.Sc. Dissertation, Utah State University, Utah, USA.
- Roussis, P.C. (2009), "Study on the effect of uplift-restraint on the seismic response of base-isolated structures", *J. Struct. Eng.*, **135**(12), 1462-1471, [https://doi.org/10.1061/\(ASCE\)ST.1943-541X.0000070](https://doi.org/10.1061/(ASCE)ST.1943-541X.0000070).
- Ala Saadeghvaziri, M., Feizi, B., Kempner Jr., L. and Alston, D. (2009), "On seismic response of substation equipment and application of base isolation to transformers", *IEEE Transactions on Power Delivery*, **25**(1), 177-186, <https://doi.org/10.1109/TPWRD.2009.2033971>.
- Schiff, A.J. (1998), *Guide to Improved Earthquake Performance of Electric Power Systems*, American Society of Civil Engineers, VA, Reston, USA.
- Stearns, C.C. and Filiatrault, A. (2005), *Electrical Substation Equipment Interaction: Experimental Rigid Conductor Studies*, Pacific Earthquake Engineering Research Center, USA.
- Tavanir (1990), "Damage report of Shahid Beheshti power plant in 1990 earthquake", Tavanir, Tehran, Iran.
- Vamvatsikos, D. and Cornell, C.A. (2002), "Incremental dynamic analysis", *Earthq. Eng. Struct. Dynam.*, **31**(3), 491-514, <https://doi.org/10.1002/eqe.141>.
- Wang, L., Oua, Jin, Liu, Weiqing and Wang, Shuguang (2013), "Full-scale tests and analytical model of the Teflon-based lead rubber isolation bearings", *Struct. Eng. Mech.*, **48**(6), 809-822, <https://doi.org/10.12989/SEM.2013.48.6.809>.
- Warn, G.P. and Ryan, K.L. (2012), "A review of seismic isolation for buildings: historical development and research needs", *Buildings*, **2**(3), 300-325, <https://doi.org/10.3390/buildings2030300>.
- Waseem, M. and Spacone, E. (2017), "Fragility curves for the typical multi-span simply supported bridges in northern Pakistan", *Struct. Eng. Mech.*, **64**(2), 213-223, <https://doi.org/10.12989/sem.2017.64.2.213>.
- Wen, B., Zhang, J. and Niu, D. (2004), "Application of isolation technology in high-voltage electrical equipments", *The 14th World Conference on Earthquake Engineering*, Beijing, China.
- Yang, Z. and Lam, E.S. (2015), "Seismic mitigation of an existing building by connecting to a base-isolated building with viscoelastic dampers", *Struct. Eng. Mech.*, **53**(1), 57-71, <https://doi.org/10.12989/SEM.2015.53.1.057>.
- Yue, H., Chen, J. and Xu, Q. (2019), "Optimal design of multiple annular tuned liquid dampers for seismic reduction of 1,100-kV composite bushing", *Struct. Control Health Monitor.*, **26**(4), e2316, <https://doi.org/10.1002/stc.2316>.
- Zayas, V.A., Low, S.S. and Mahin, S.A. (1990), "A simple pendulum technique for achieving seismic isolation", *Earthq. Spectra*, **6**(2), 317-333, <https://doi.org/10.1193/1.1585573>.
- ASCE 7-05, (2005), *Minimum Design Loads for Buildings and Other Structures*, American Society of Civil Engineers, VA, Reston, USA.